A Study of the Unimolecular Dissociation of the 2-Buten-2-yl Radical via the 193 nm Photodissociation of 2-Chloro-2-butene

ARTICLE *in* THE JOURNAL OF PHYSICAL CHEMISTRY A · AUGUST 2005

Impact Factor: 2.69 · DOI: 10.1021/jp050970e · Source: PubMed

5 AUTHORS, INCLUDING:

Laura R McCunn
Marshall University
20 PUBLICATIONS **422** CITATIONS
SEE PROFILE

Laurie J Butler
University of Chicago
93 PUBLICATIONS **2,406** CITATIONS
SEE PROFILE

Jinian Shu
Chinese Academy of Sciences
77 PUBLICATIONS **901** CITATIONS
SEE PROFILE

A Study of the Unimolecular Dissociation of the 2-Buten-2-yl Radical via the 193 nm Photodissociation of 2-Chloro-2-butene

Laura R. McCunn, Maria J. Krisch, Yi Liu, and Laurie J. Butler*

The James Franck Institute and Department of Chemistry, The University of Chicago, Chicago, Illinois 60637

Jinian Shu

Chemical Sciences Division, Lawrence Berkeley National Laboratory, Berkeley, California 94720

Received: February 24, 2005; In Final Form: May 12, 2005

This work investigates the unimolecular dissociation of the 2-buten-2-yl radical. This radical has three potentially competing reaction pathways: C−C fission to form CH_3 + propyne, C−H fission to form H + 1,2-butadiene, and C−H fission to produce H + 2-butyne. The experiments were designed to probe the branching to the three unimolecular dissociation pathways of the radical and to test theoretical predictions of the relevant dissociation barriers. Our crossed laser-molecular beam studies show that 193 nm photolysis of 2-chloro-2-butene produces 2-buten-2-yl in the initial photolytic step. A minor C−Cl bond fission channel forms electronically excited 2-buten-2-yl radicals and the dominant C−Cl bond fission channel produces ground-state 2-buten-2-yl radicals with a range of internal energies that spans the barriers to dissociation of the radical. Detection of the stable 2-buten-2-yl radicals allows a determination of the translational, and therefore internal, energy that marks the onset of dissociation of the radical. The experimental determination of the lowest-energy dissociation barrier gave 31 ± 2 kcal/mol, in agreement with the 32.8 ± 2 kcal/mol barrier to C−C fission at the G3//B3LYP level of theory. Our experiments detected products of all three dissociation channels of unstable 2-buten-2-yl as well as a competing HCl elimination channel in the photolysis of 2-chloro-2-butene. The results allow us to benchmark electronic structure calculations on the unimolecular dissociation reactions of the 2-buten-2-yl radical as well as the CH_3 + propyne and H + 1,2-butadiene bimolecular reactions. They also allow us to critique prior experimental work on the H + 1,2-butadiene reaction.

Introduction

This paper investigates the dissociation dynamics of the 2-buten-2-yl radical, produced by the 193 nm photodissociation of 2-chloro-2-butene. This radical serves as the intermediate along the reaction coordinate for the combination of the methyl radical with propyne and the reaction of the H atom with 2-butyne. It is one of several radical intermediates in the bimolecular H + 1,2-butadiene reaction. The 2-buten-2-yl radical is one of several straight-chain isomers of the C_4H_7 unsaturated hydrocarbon radical species. Several groups[1−3] have sought to characterize the important dissociation and isomerization channels of the C_4H_7 radical isomers. Previous electronic structure G3//B3LYP calculations in our group[3] have characterized the relative energies and isomerization barriers of the C_4H_7 radical isomers, as well as the enthalpies and transition states for the available dissociation reactions of the radicals (Figure 1). Listed below are the reactions that are energetically possible for 2-chloro-2-butene at 193 nm, with the dissociation pathways open to the 2-buten-2-yl radicals and the C−C fission pathways open to the HCl elimination cofragments indented. Enthalpies for reactions 1, 5, and 7 were not found in the literature, so we used G2M(RCC, MP2) and G2M(RCC6) methods[4] in Gaussian 98[5] for reaction 1 and QCISD(T)//6-31G(d) for 5 and 7. The uncertainties in these calculations are expected to be no greater than 1.5 kcal/mol

$$CH_3C(Cl)CHCH_3 \rightarrow CH_3\dot{C}{=}CHCH_3 + Cl \qquad \Delta H_{0K} = 93.5 \text{ kcal/mol} \quad (1)$$

$$\text{cis-}CH_3\dot{C}{=}CHCH_3 \rightarrow CH_3C{\equiv}CH + CH_3 \qquad \Delta H_{0K} = 22.7 \text{ kcal/mol}^3 \quad (2)$$

$$\text{cis-}CH_3\dot{C}{=}CHCH_3 \rightarrow CH_2{=}C{=}CHCH_3 + H \qquad \Delta H_{0K} = 35.4 \text{ kcal/mol}^3 \quad (3a)$$

$$\text{trans-}CH_3\dot{C}{=}CHCH_3 \rightarrow CH_2{=}C{=}CHCH_3 + H \qquad \Delta H_{0K} = 36.2 \text{ kcal/mol}^3 \quad (3b)$$

$$\text{trans-}CH_3\dot{C}{=}CHCH_3 \rightarrow CH_3C{\equiv}CCH_3 + H \qquad \Delta H_{0K} = 32.3 \text{ kcal/mol}^3 \quad (4)$$

$$CH_3C(Cl)CHCH_3 \rightarrow CH_2{=}C{=}CHCH_3 + HCl \qquad \Delta H_{0K} = 37 \text{ kcal/mol} \quad (5)$$

$$CH_2{=}C{=}CHCH_3 \rightarrow CH_2{=}C{=}\dot{C}H + CH_3 \qquad \Delta H_{0K} = 77.8 \text{ kcal/mol}^6 \quad (6)$$

$$CH_3C(Cl)CHCH_3 \rightarrow CH_3C{\equiv}CCH_3 + HCl \qquad \Delta H_{0K} = 34 \text{ kcal/mol} \quad (7)$$

$$CH_3C{\equiv}CCH_3 \rightarrow CH_2{=}C{=}\dot{C}H + CH_3 \qquad \Delta H_{0K} = 81.3 \text{ kcal/mol}^6 \quad (8)$$

* Corresponding author. E-mail: L-Butler@uchicago.edu.

10.1021/jp050970e CCC: $30.25
Published on Web 06/30/2005

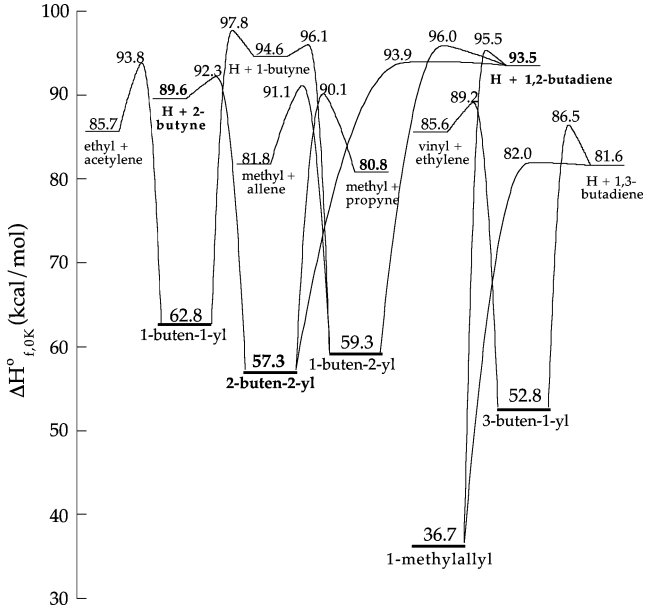

Figure 1. Minima and transition states (corrected for ZPE) calculated at the G3//B3LYP level of theory for the important isomerization and dissociation channels of the straight-chain C_4H_7 radical isomers. Reproduced with permission from *J. Phys. Chem. A* **2004**, *108*, 2268−2277.

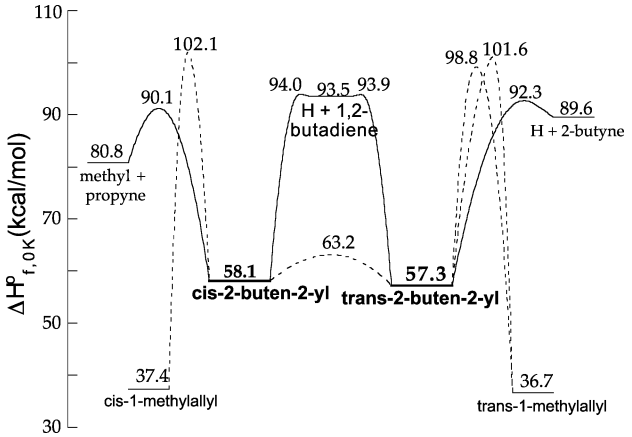

Figure 2. G3//B3LYP predictions of dissociation barriers and product energies for the ground-state dissociation of cis- and trans- 2-buten-2-yl radicals. Reproduced with permission from *J. Phys. Chem. A* **2004**, *108*, 2268−2277.

There has been interest in the mechanisms of isomerization of the C_4H_7 radicals,[1,7,8] especially with regard to ring opening. Matheu et al. mapped out an estimated potential energy surface for the C_4H_7 system in their study of the H + cyclobutene reaction using group additivity rules for the purpose of calculating rate constants.[1] They included the five straight-chain C_4H_7 isomers, as well as cyclic isomers and all possible dissociation products. For the H + cyclobutene system, 3-buten-1-yl and the cyclobutyl radical were predicted to be the only significant isomers produced. The isomerization of 2-buten-2-yl to 1-methylallyl has been predicted to have a higher barrier than the dissociation channels 2−4 and a less entropically favored transition state, so it should not contribute appreciably to the product branching.[3] In this study of 2-buten-2-yl, we consider only the calculated reaction enthalpies and barriers with zero-point corrections, shown in Figure 2, on the C_4H_7 potential energy surface. The results presented in Figure 3 of the paper by Matheu et al. appear similar, though the C−C fission pathway to methyl + propyne is mislabeled as H + propyne.

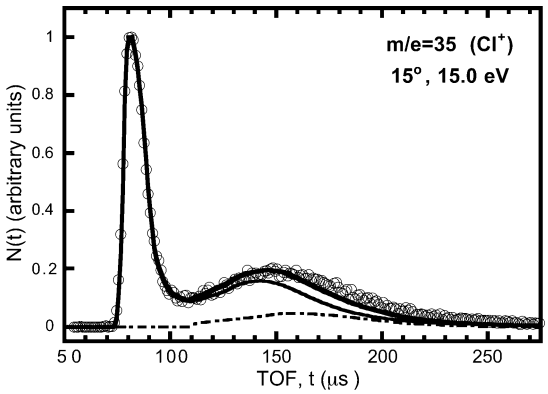

Figure 3. Time-of-flight (TOF) spectrum of $m/e = 35$ (Cl^+) from the photodissociation of 2-chloro-2-butene at 193 nm. Open circles represent experimental data taken at a source angle of 15° and ionization energy of 15.0 eV for 25,000 laser shots. The thin solid line is the forward convolution fit to the data with the $P(E_T)$ shown in Figure 4. The dot−dashed line represents signal purported to be from clusters in the molecular beam, as reasoned from the fitting of Figures 5 and 15. The bold solid line is the total fit.

There is a scarcity of experimental data on the 2-buten-2-yl radical, perhaps because it is not the lowest-energy C_4H_7 isomer. Yet it is the key radical intermediate in the reaction of CH_3 + propyne and in the reaction of H + 2-butyne, as well as one of several possible intermediates in the reaction of H + 1,2-butadiene. In one relevant study, Getty et al. measured rate constants for the addition of methyl to propyne at 106−192 °C and found that the methyl radical added to the terminal carbon with >90% efficiency to make the 2-buten-2-yl radical.[9] Measured Arrhenius parameters were $\log A = 11.7$ c.c.mol^{-1} s^{-1} and $E_a = 8.8$ kcal/mol. This agrees, within error, with the G3//B3LYP value of 9.3 kcal/mol for the exit barrier of the CH_3 + propyne channel.[3]

The experiments described herein utilize 2-chloro-2-butene, $CH_3C(Cl)CHCH_3$, as a photolytic precursor for the radical. The experiments measure the velocity distributions of the nascent 2-buten-2-yl radical and its subsequent dissociation products. The goals of our experiments are to monitor product branching in the unimolecular dissociation of the 2-buten-2-yl radical as a function of its energy and also to provide an experimental test for the various theoretical predictions of the 2-buten-2-yl potential energy surface described above.

Experimental Method

Photofragment translational spectroscopy was performed on the rotating-source crossed laser-molecular beam apparatus on the Chemical Dynamics Beamline at Lawrence Berkeley National Laboratory's Advanced Light Source (ALS). Details of the experimental apparatus have been described previously.[10,11] A 9.4% 2-chloro-2-butene-He molecular beam was created by bubbling He (650 Torr total backing pressure) through 2-chloro-2-butene (cis and trans mixture, 97% purity, Narchem) cooled to 6 °C and expanding it through a piezoelectric pulsed valve (0.5 mm orifice) operating at 100 Hz. The nozzle was heated to temperatures between 40 and 80 °C (the exact value varied from day to day) to reduce cluster formation. The molecular beam of the parent molecule was characterized by directing the beam through a chopper wheel along the detector axis. The measured number-density speed distribution of the 2-chloro-2-butene molecular beam for the data presented here was typically peaked at 1.3×10^5 cm/s with a full-width at half-maximum of 7%.

Photodissociation was accomplished with a GAM excimer laser operating at the 193.3 nm ArF transition and a pulse energy of 10 mJ/pulse. The laser ran at 50 Hz for shot-to-shot (molecular beam on, laser off) background subtraction. The laser beam was focused to an area of 2.4 mm × 4.3 mm, intersecting the molecular beam at a 90° angle in the interaction region. Photofragments recoiling in the direction of the detector traveled 15.1 cm to the ionizing region, where tunable VUV synchrotron radiation ionized a portion of the fragments. Photoionization energies were selected by tuning the gap of a U10 undulator, which generated the radiation. The necessary undulator gap (mm) was calculated from the desired photoionization energy, x (eV), using the following polynomial:[12]

$$\text{gap(mm)} = 7.875\text{(mm)} + 2.5054\text{(mm/eV)}x - 0.068545\ \text{(mm/eV}^2)x^2 + 0.00082477\text{(mm/eV}^3)x^3$$

For example, Cl^+ data at $m/e = 35$ were collected using an 15.0 eV photoionization energy, requiring a 32.817 mm undulator gap. Unwanted higher harmonics of VUV radiation were removed by a rare gas filter, and at photon energies below 10.8 eV, by a MgF_2 window. The VUV beam was defined by slits that were varied from 10 mm × 10 mm to 5 mm × 5 mm.

Ionized photofragments were mass-selected by an Extrel 2.1 MHz quadrupole mass spectrometer and then counted by a Daly detector. A multichannel scaler was used to record the total time-of-flight (TOF) of the photofragments from the interaction region to the detector. Recoil translational energy distributions were found by forward convolution fitting of the TOF spectra. The forward convolution fitting of the data takes into account the ion flight time, derived from the machine's ion flight constant of 5.78 $\mu s \cdot amu^{-1/2}$. The experimental data and fits shown in this paper have already subtracted the 5.5 μs delay between the trigger of the multichannel scaler and the arrival of the laser pulse at the interaction region.

Supplemental data were taken on the crossed laser-molecular beam apparatus in the Chicago lab,[13] which is similar to the ALS apparatus. Only the major differences between the Chicago and ALS apparatuses are described here. A molecular beam was formed by expanding a mixture of He (300 Torr total backing pressure) and 2-chloro-2-butene cooled to −10.5 °C through a CW nozzle (0.09 mm orifice). The nozzle was heated to approximately 300 °C, which was found to prevent any cluster formation in the molecular beam. The flight path length from the laser interaction region to the detector was 44.21 cm, and photofragments were ionized by a 200-eV electron bombardment ionizer instead of VUV radiation. An ion flight constant of 4.5 $\mu s \cdot amu^{-1/2}$ was used for fitting data from this instrument. All figures in this paper present data from the ALS, unless noted as Chicago lab data (Figure 5).

Results and Analysis

The data showed that both C−Cl bond fission and HCl elimination occur in the photodissociation of 2-chloro-2-butene at 193 nm. C−Cl fission was evidenced by Cl^+ signal at $m/e = 35$ shown in Figure 3. The total recoil kinetic energy distribution $P(E_T)$ in C−Cl fission was determined by forward convolution fitting of the data and is shown by the solid line in Figure 4. The total $P(E_T)$ is bimodal, with the low-energy component peaking below 1 kcal/mol. Our results presented here suggest that the low kinetic energy C−Cl bond fission channel produces 2-buten-2-yl radicals in an excited electronic state, while the dominant, high kinetic energy, C−Cl bond fission channel produces 2-buten-2-yl radicals in the ground electronic state.

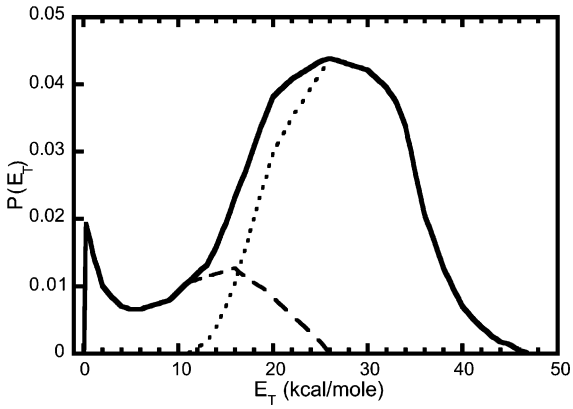

Figure 4. Recoil kinetic energy distribution in C−Cl bond fission. The solid line shows the total $P(E_T)$. The total $P(E_T)$ is divided into two subdistributions used in fitting subsequent spectra. The dotted line corresponds to high E_T, low E_{int} C_4H_7 radicals that are stable to dissociation. The dashed line shows high E_{int}, unstable C_4H_7 radicals.

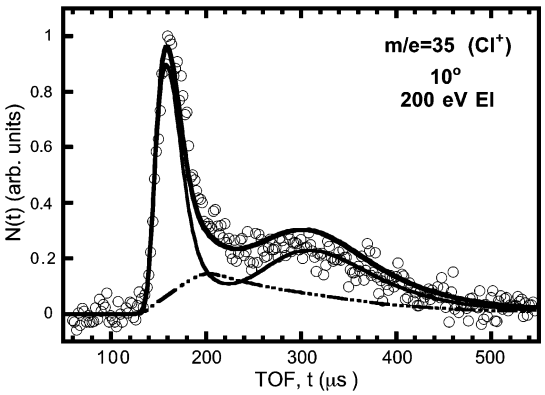

Figure 5. TOF spectrum of $m/e = 35$ (Cl^+), 10° source angle, obtained from 500 000 laser shots on the Chicago apparatus with electron-bombardment (EI) ionization. This spectrum exhibits no signal from clusters. Open circles are experimental data, and the bold solid line is the total fit. The thin solid line is the fit to the data using the total $P(E_T)$ shown by the solid line in Figure 4. The broken line shows a contribution from HCl that undergoes dissociative ionization and appears at $m/e = 35$, fit by the $P(E_T)$ in Figure 8.

The low kinetic energy portion of the $P(E_T)$ fits only a portion of the low velocity Cl^+ signal. The remaining low velocity signal is attributed to cluster fragments, shown by the dot−dashed line in Figure 3. To verify that the signal is due to clusters, we used the $P(E_T)$ in Figure 4 to fit Cl^+ data collected on the Chicago apparatus. These data were taken using a nozzle temperature of 300 °C, and it was determined that no appreciable signal from clusters was present. The data and the fit are shown in Figure 5.

Stable 2-buten-2-yl radicals were observed in a $m/e = 55$ TOF spectrum. (Figure 6) The data were fit by using a high kinetic energy portion of the C−Cl bond fission $P(E_T)$, shown by the dotted line in Figure 4. Only the higher kinetic energy part of the total C−Cl bond fission $P(E_T)$ is used, as the Cl atoms with low recoil kinetic energy correspond to C_4H_7 radicals with internal energies sufficient to overcome the barrier to dissociation, meaning they would not be detected at $m/e = 55$. The unstable radicals were formed from C−Cl bond fission imparting lower recoil kinetic energies to the two fragments as shown by the portion of the E_T distribution marked by the dashed line in Figure 4. (Note that this portion of the $P(E_T)$ represents unstable radicals assigned to both the ground and excited states.) The E_T marking the onset of dissociation of the unstable 2-buten-2-yl radicals, 26 ± 1 kcal/mol, provides an

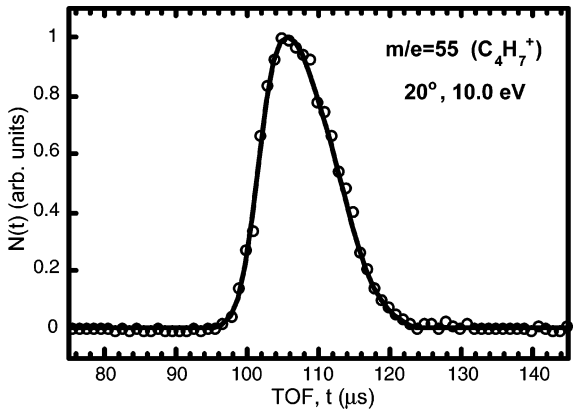

Figure 6. TOF spectrum of $m/e = 55$ ($C_4H_7^+$) taken at a 20° source angle and 10.0 eV ionization energy for 50 000 shots. Open circles are experimental data points and the solid line is the fit to the data obtained from the subdistribution of the C−Cl bond fission $P(E_T)$ shown by the dotted line in Figure 4. This portion of the total $P(E_T)$ corresponds to C_4H_7 radicals with high E_T, and hence low E_{int}, that cannot overcome the dissociation barrier and are detected at $m/e = 55$.

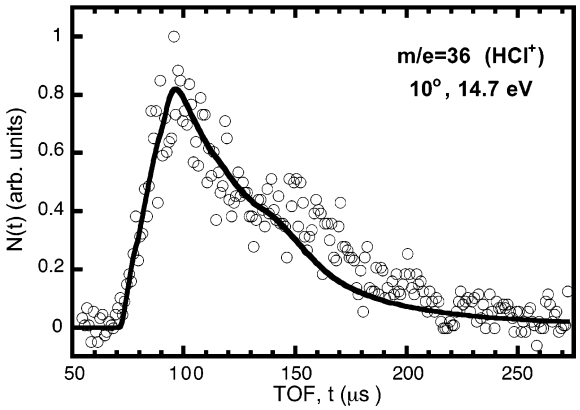

Figure 7. TOF spectrum of $m/e = 36$ (HCl^+) obtained from 150 000 laser shots at a 10° source angle and 14.7 eV ionization energy. Open circles are experimental data and the solid line is the forward convolution fit to the data, with $P(E_T)$ shown in Figure 8.

experimental determination of the lowest-energy barrier to dissociation of these radicals, as described in the Discussion. A substantially worse fit is obtained by extending the onset to $E_T = 27$ kcal/mol or truncating it at 25 kcal/ mol.

A TOF spectrum taken at $m/e = 36$ ($H^{35}Cl^+$) and a 10° source angle (Figure 7) indicated the presence of an HCl elimination channel. The data were fit by a single $P(E_T)$, shown by the bold solid line in Figure 8. This $P(E_T)$ is divided approximately into two distributions to show HCl products that have C_4H_6 cofragments predicted to be stable (thin dotted line) and C_4H_6 with internal energy sufficient for secondary dissociation (thin solid line). The division of the $P(E_T)$ is only an estimate, as we are unable to measure the internal energy of HCl molecules following elimination to deduce the exact internal energy distribution of the C_4H_6 cofragments. The internal energies of C_4H_6 products can be found by conservation of energy:

$$E_{parent} + h\nu = \Delta H_{0K}(\text{HCl elimination}) + E_{int}(C_4H_6) + E_{int}(\text{HCl}) + E_T$$

Our QCISD(T)//6-31G(d) calculations predict that the initial HCl elimination is endothermic by 34 kcal/mol. Study of four-center HCl elimination in 2-chloropropene suggested that HCl carries away on average 18 kcal/mol in internal energy.[14] Assuming that the four-center elimination processes of 2-chloro-2-butene

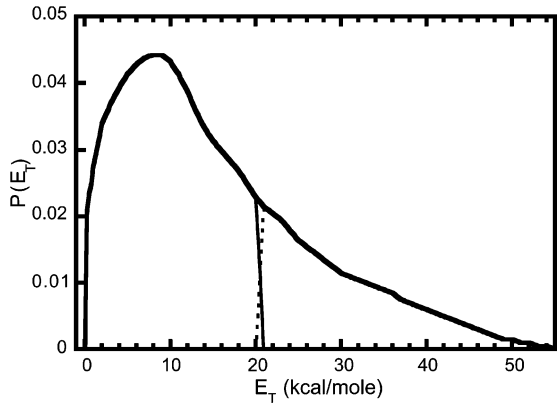

Figure 8. Distribution of recoil translational energy imparted in HCl elimination. The bold solid line shows the $P(E_T)$ used to fit the data in Figure 7. The thin dotted line shows the portion of the $P(E_T)$ corresponding to HCl elimination that produces C_4H_6 cofragments that are predicted to have internal energy below the barrier to unimolecular dissociation. The thin solid line corresponds to C_4H_6 cofragments that are predicted to be higher in energy than the dissociation barrier.

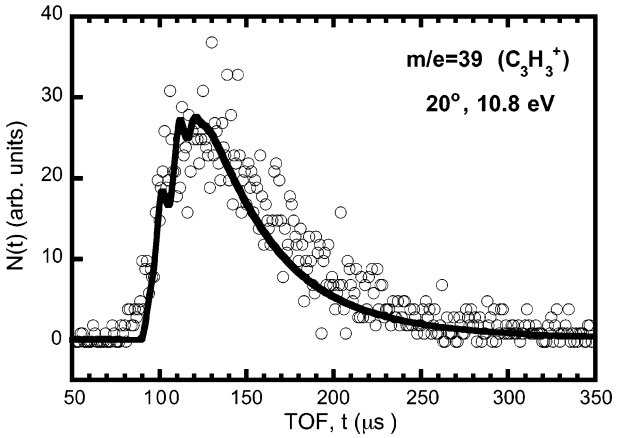

Figure 9. TOF spectrum of $m/e = 39$ ($C_3H_3^+$) obtained at a 20° source angle and 10.8 eV ionization energy after 300 000 laser shots. Open circles represent experimental data, and the solid line is the forward convolution fit to the data. $C_3H_3^+$ signal is due to propargyl radicals produced from dissociation of energetic C_4H_6 molecules originating from HCl elimination. The data were fit using the thin solid line in Figure 8, accounting for the translational energy of unstable C_4H_6 cofragments to HCl elimination, and also the recoil imparted to the recoiling propargyl and methyl fragments, as demonstrated by the $P(E_T)$ in Figure 10.

are similar to those of 2-chloropropene, we use $E_{int}(\text{HCl}) = 18$ kcal/mol and a G2M(CC,MP2) predicted dissociation barrier of $E_{int} = 77.8$ kcal/mol[6] to posit that C_4H_6 from elimination events of $E_T \geq 20$ kcal/mol do not dissociate appreciably. This gives a satisfactory fit to our $m/e = 39$ and 54 data, as described below.

A TOF spectrum taken at $m/e = 39$ was assigned to propargyl radicals produced from the dissociation of C_4H_6 cofragments to HCl elimination as shown in reaction 6 or 8. Note that 2-butyne can isomerize to 1,2-butadiene at energies lower than the barrier for 1,2-butadiene to dissociate to CH_3 + propargyl.[6] Figure 9 shows the experimental data and a forward convolution fit. The fit accounts for the velocity imparted to the C_4H_6 molecule in the initial HCl elimination, as described by the low kinetic-energy portion (thin solid line) of Figure 8, as well as the velocity imparted during the recoil of the propargyl radical from the methyl radical in the dissociation of C_4H_6. The energy imparted in the second step can be described by the distribution shown in Figure 10. The $P(E_T)$ peaks at 3 kcal/mol, but a nearly

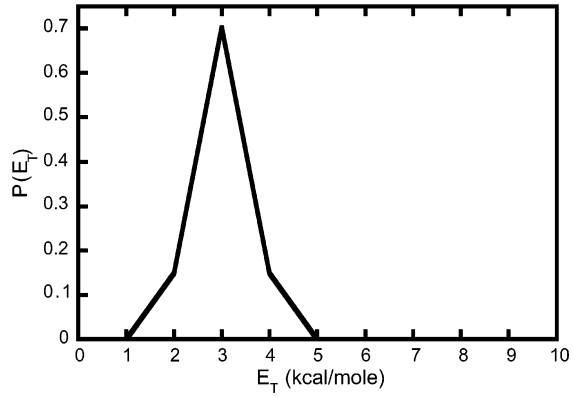

Figure 10. Recoil translational energy distribution for $C_4H_6 \rightarrow C_3H_3 + CH_3$ from the higher internal energy coproduct of HCl elimination step. This $P(E_T)$ is used to fit the data in Figure 9.

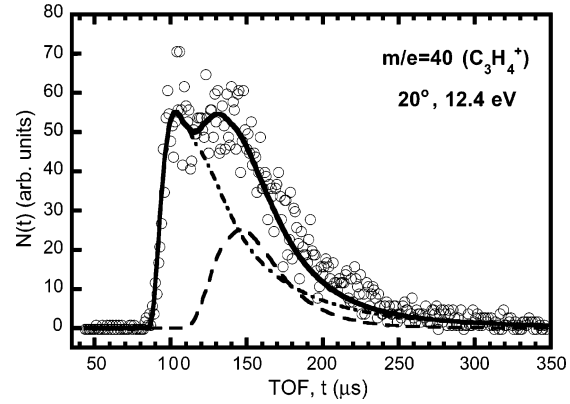

Figure 11. TOF spectrum of $m/e = 40$ ($C_3H_4^+$) at a 20° source angle and 12.4 eV ionization energy after 300 000 laser shots. Open circles are experimental data, and the solid line is the overall fit to the data. The signal shown by the dashed and dot−dashed lines is attributed to propyne produced in the dissociation of unstable C_4H_7 radicals and is fit by the $P(E_T)$ distributions in Figures 12−14 as described in the Results and Analysis.

identical fit to the data could also be obtained with the $P(E_T)$ shifted to peak at 4 kcal/mol. A $P(E_T)$ peaking at 2 kcal/mol, however, underfit the data on both the rising and falling edges of the TOF spectrum.

Propyne products from the dissociation of 2-buten-2-yl radicals were evidenced in the $m/e = 40$ TOF spectrum. (Figure 11) The forward convolution fit accounts for the recoil of the C_4H_7 radical and Cl atom in the initial photolytic step, as well as the recoil of the methyl and propyne fragments in the dissociation of the radical. The low-energy portion (dashed line) of the C−Cl bond fission $P(E_T)$ in Figure 4 was used in fitting the data. Notably, the best fit to the data required that this $P(E_T)$, corresponding to C−Cl bond fission producing unstable 2-buten-2-yl radicals, be divided into two distributions (Figure 12) with a different $P(E_T)$ constructed to describe the translational energy imparted in the subsequent dissociation of the radicals in each of the distributions shown in Figure 12. The dashed line in Figure 12 is assigned to 2-buten-2-yl radicals formed in the excited state, while the dot−dashed line is assigned to ground-state radicals. The two $P(E_T)$ distributions corresponding to reaction 2 are found in Figures 13 and 14. Referring back to Figure 11, the signal contribution outlined by the dashed line shows propyne that came from excited-state 2-buten-2-yl radicals from initial photolysis events with $0 < E_T < 8$ kcal/mol, as shown by the dashed line in Figure 12, and with a distribution of recoil energy imparted in the dissociation of the radical as described by the $P(E_T)$ in Figure 13. Similarly, the

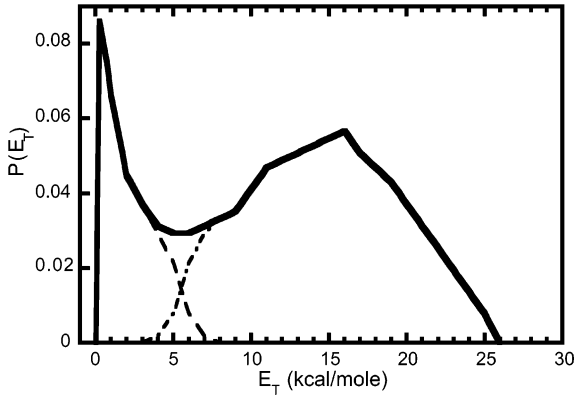

Figure 12. $P(E_T)$ in C−Cl bond fission corresponding to 2-buten-2-yl radicals that have sufficient energy to overcome the barrier to dissociation. The bold solid line shows the distribution for all unstable C_4H_7 radicals and can also be seen in Figure 4. To properly fit the data in Figure 11, this $P(E_T)$ was divided into two distributions, one representing excited-state radicals (dashed line) and another representing ground-state radicals (dot−dashed line), which were then combined with the distributions in Figures 13 and 14, respectively, that describe the velocity imparted to methyl and propyne during the dissociation of the radicals.

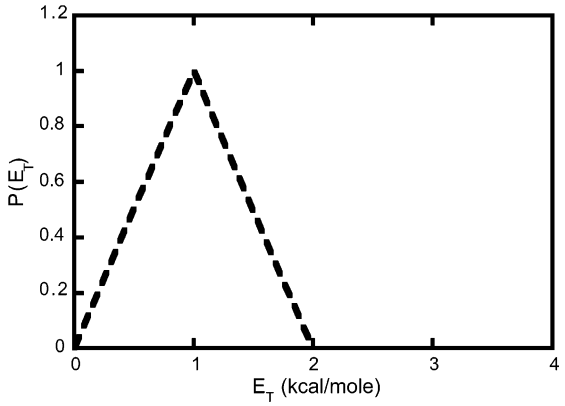

Figure 13. $P(E_T)$ describing the translational energy distribution imparted during the recoil of methyl and propyne in the dissociation of excited-state C_4H_7 radicals with the energy distribution shown by the dashed line in Figure 12. The resultant fit is shown by the dashed line in Figure 11.

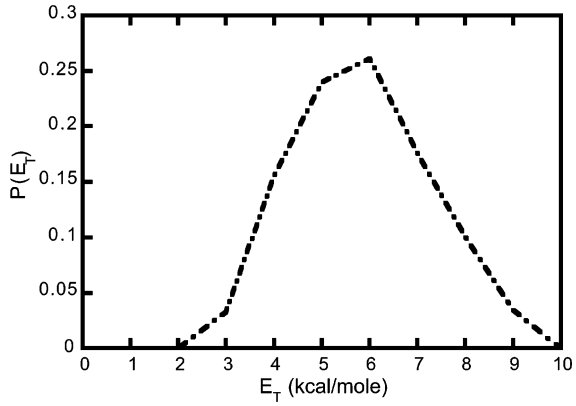

Figure 14. $P(E_T)$ describing the translational energy distribution imparted during the recoil of methyl and propyne in the dissociation of unstable ground-state C_4H_7 radicals with the energy distribution shown by the dot−dashed line in Figure 12. The resultant fit is shown by the dot−dashed line in Figure 11.

dot−dashed line in Figure 11 shows the signal from propyne produced from reactions 1 and 2, via ground-state radicals, with translational recoil energy distributions described by the dot−

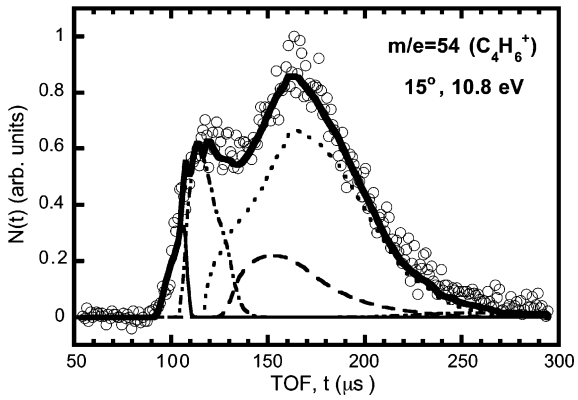

Figure 15. Experimental $m/e = 54$ ($C_4H_6^+$) TOF taken at a 15° source angle and 10.8 eV ionization energy for 300 000 laser shots. Open circles are experimental data points and the bold solid line is the total fit to the data. The thin solid line shows the contribution from C_4H_6 cofragments to HCl elimination with predicted internal energy below the barrier to dissociation. The thin dotted line in Figure 8 shows the $P(E_T)$ for these fragments. The dot−dashed line shows C_4H_6 products from the H-loss channels of unstable C_4H_7 radicals formed in the ground state. The long-dashed line corresponds to C_4H_6 products from the H-loss channels of excited-state C_4H_7 radicals. The C−H bond fission channels of the C_4H_7 radicals were fit by $P(E_T)$ distributions for ground-state radicals, shown by the dot−dashed line in Figure 12, and excited-state radicals, shown by the long-dashed line in Figure 12. The remaining signal is attributed to clusters, shown by the dotted line.

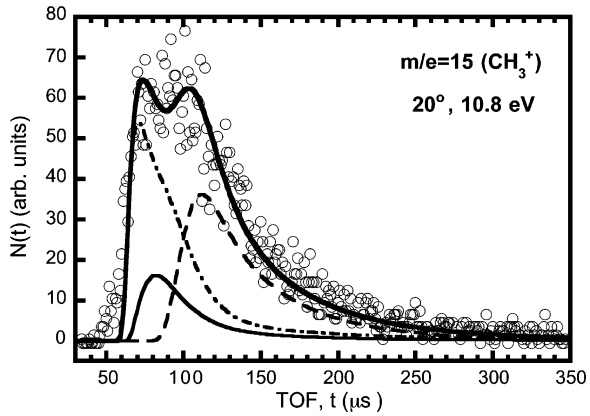

Figure 16. Experimental TOF of $m/e = 15$ (CH_3^+) at a 20° source angle and 10.8 eV ionization energy after 500 000 laser shots. Open circles are experimental data points and the bold solid line is the total fit to the data. All contributions to the fit are derived from momentum-matching to experimental data of $m/e = 40$ and 39. The long-dashed and dot−dashed lines correspond to those of Figure 11. The thin solid line shows methyl radicals formed in conjunction with propargyl radicals as shown in Figure 9.

dashed lines in Figures 12 and 14, respectively. Comparing the areas of the distributions shown in Figure 12 shows that the ground-state 2-buten-2-yl radicals are formed in a 3:1 ratio to the excited-state radicals, however, assuming the same ratio in C−C fission of these radicals does not give a good fit. These two component $P(E_T)$'s may be used in a calculation of the propyne signal in Figure 11, correcting for the appropriate kinematic factors and Jacobians to go from the 3:1 ratio of reactant ground- to excited-state radicals to the final relative signal levels in Figure 11. If we assume both the ground and excited state radicals are equally likely to produce propyne + CH_3, we underfit the fast (dot−dashed) signal in Figure 11. The good fit shown is obtained by assuming that the propyne products originate from 2-buten-2-yl radicals in the ground-state/excited-state ratio of 5:1; this shows there is an enhanced probability of C−C fission for ground-state 2-buten-2-yl.

Both C−Cl bond fission and HCl elimination channels in 2-chloro-2-butene contribute to the $m/e = 54$ ($C_4H_6^+$) TOF spectrum. Some of the unstable C_4H_7 radicals, found in C−Cl photodissociation events with the portion of the $P(E_T)$ represented by the dashed line in Figure 4, may access one of the available H-loss channels, reactions 3a,b and 4, to produce 2-butyne or 1,2-butadiene. Loss of a hydrogen will not significantly change the velocity of the radical, so the TOF distribution of the C_4H_6 products can be predicted by using the $P(E_T)$ for their parent C_4H_7 radicals. HCl elimination from 2-chloro-2-butene directly produces C_4H_6 by reactions 5 and 7. A fraction of both the resultant 2-butyne and the 1,2-butadiene products dissociate predominantly to propargyl + CH_3 at the energies available in this experiment. It also happens that $C_4H_6^+$ is a dominant daughter ion fragment of 2-chloro-2-butene, so it is possible for cluster fragments and stable C_4H_7 radicals to dissociatively ionize and appear at $m/e = 54$. We were unable to collect data at parent mass ($m/e = 90$) to confirm the presence of clusters. Taking all of these facts into consideration, the fitting of the $m/e = 54$ spectrum is not uniquely determined.

Figure 15 shows a fit of $m/e = 54$ data using the low recoil kinetic energy portion of the C−Cl bond fission $P(E_T)$ which corresponds to 2-buten-2-yl radicals that could possibly dissociate to C_4H_6. The dot−dashed line corresponds to C_4H_6 produced by C−H fission of ground-state 2-buten-2-yl radicals. C_4H_6 products originating from excited-state 2-buten-2-yl radicals are shown by the long-dashed line. The $P(E_T)$ distributions in Figure 12 were used in fitting the data, although the underdetermined nature of the $m/e = 54$ data prohibits us from determining the ratio of C_4H_6 products from the ground and excited states of 2-buten-2-yl. Although our experimentally determined lowest barrier to dissociation of the 2-buten-2-yl radical most likely corresponds to reaction 2, which does not produce C_4H_6, the barriers to reactions 3a,3b and 4 are predicted to be only 2−4 kcal/mol higher. Truncating the low E_T portion of the C−Cl fission $P(E_T)$ by 4 kcal/mol would not drastically alter the fit in Figure 15. The thin solid line in Figure 15 shows the distribution of C_4H_6 cofragments to HCl elimination with insufficient internal energy to overcome the barriers to dissociation in reaction 6 or 8. In the TOF spectrum of Figure 15, there is very high signal in the range of 125−300 μs that cannot be accounted for by any photodissociation events. We attribute this signal to clusters and show the possible contribution with a dotted line.

Thus far, we have postulated the appearance of signal from molecular clusters in both $m/e = 54$ and 35 TOF spectra. It is reasonable to expect that the only difference in the two cluster signal distributions should be in their ion flight times. To test the validity of our claim regarding the existence of clusters in our data, we took the cluster signal peak constructed for Figure 15 and used the ion flight constant to predict where the same cluster signal would appear in a $m/e = 35$ TOF spectrum taken at the same angle for the rotating source. The time-shifted and appropriately scaled cluster signal could account for the suspected cluster signal at $m/e = 35$. The dot−dashed line in the $m/e = 35$ TOF spectrum of Figure 3 shows the fit using the cluster signal from Figure 15.

Figure 16 shows data collected at $m/e = 15$ and includes the momentum-matched partner to propyne in reaction 2. The dashed line and dot−dashed line are momentum-matched to the corresponding lines in Figure 11, fit in the same manner as described above for the $m/e = 40$ TOF spectrum with the $P(E_T)$ distributions shown in Figures 12, 13 and 14. The solid line marks the distribution of CH_3 radicals produced in conjunction with propargyl radicals in reaction 6 or 8. This signal is

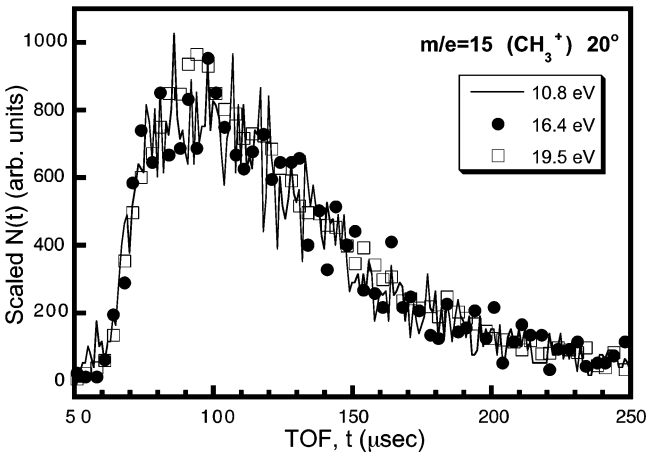

Figure 17. Overlaid $m/e = 15$ (CH_3^+), 20° source angle, TOF spectra taken at ionization energies of 10.8, 16.4, and 19.5 eV for 500 000, 300 000, and 200 000 laser shots, respectively. The data have been scaled to the same height for purpose of comparison. No difference can be seen in the shape of the three TOF distributions, making it impossible to calculate a branching ratio among reactions 2, 3a,b and 4.

momentum-matched to that of the $m/e = 39$ TOF spectrum in Figure 9, using the $P(E_T)$s in Figures 8 and 10.

Though the dot−dashed line contribution to the $m/e = 54$ TOF spectrum in Figure 15 clearly evidences C_4H_6 products from dissociation of radicals by reactions 3a,3b and 4, the photoionization energies of 2-butyne and 1,2-butadiene are too close to distinguish these isomers with the moderate resolution afforded in these experiments. We did, however, attempt to distinguish them by their daughter cracking to $m/e = 15$. The ionization energy of CH_3 is 9.84 eV, while the appearance energy of CH_3^+ from 1,2-butadiene is 14.4 eV and from 2-butyne is 17.6 eV.[15] Therefore, by simply tuning the ALS undulator gap to produce different ionization energies and taking $m/e = 15$ TOF spectra at each energy, it is theoretically possible to distinguish the three unimolecular dissociation channels of 2-buten-2-yl shown in reactions 2, 3a,3b and 4. We collected consecutive $m/e = 15$ spectra with a molecular beam source angle of 20° at 10.8, 16.4, and 19.5 eV. The three spectra are shown scaled and overlaid in Figure 17. There is no difference in the shapes of the spectra. This indicates that there was no significant contribution from CH_3^+ from 1,2-butadiene or 2-butyne as the ionization energy increased. This is not unexpected, since the CH_3 + propyne channel is expected to be heavily favored over reactions 3a,3b and 4, so it comprises the majority of the signal in Figure 16.

We used RRKM theory[16] to calculate rate constants for the three dissociation channels of 2-buten-2-yl for energies between 32 and 54 kcal/mol, which correspond to the internal energy range of unstable, ground-state radicals. The calculations used vibrational frequencies and rotational constants for the radical and transition states taken from the Supporting Information of ref 3. Table 1 reports the results of RRKM calculations when the external moments of inertia are treated as adiabatic and the torsional modes associated with rotation of the methyl groups are not treated as free internal rotors. At radical internal energies near the H atom channel barrier, the CH_3 + propyne channel is expected to dominate. At higher internal energies (∼10 kcal/mol above the H atom channel barrier and ∼13 kcal/mol above the C−C bond fission barrier), the RRKM calculations predict that the contribution of the H atom channel grows in significance, but the CH_3 + propyne channel still dominates. If one treated the two lowest orthogonal vibrational frequencies at the

TABLE 1: RRKM Predictions of 2-Buten-2-yl → CH_3 + Propyne Product Branching[a,b] at 300 K

radical internal energy E (kcal/mol)	$k_2(E)/[k_2(E) + k_{3a}(E) + k_{3b}(E) + k_4(E)]$	$k_2(E)/[k_2(E) + k_4(E)]$
32.1	1	1
33.1	1	1
34.1	1	1
35.1	0.999	0.999
36.1	0.997	0.997
37.1	0.995	0.996
38.1	0.992	0.994
39.1	0.990	0.993
40.1	0.987	0.992
41.1	0.985	0.990
42.1	0.982	0.989
43.1	0.979	0.988
44.1	0.977	0.986
45.1	0.974	0.985
46.1	0.972	0.984
47.1	0.969	0.983
48.1	0.967	0.982
49.1	0.965	0.981
50.1	0.962	0.979
51.1	0.960	0.978
52.1	0.957	0.977
53.1	0.955	0.977
54.1	0.953	0.976

[a] The label n in k_n label corresponds to reaction n from the Introduction. [b] Because cis/trans isomerization is fast, each of the absolute rate constants should be roughly doubled, but the ratios are unchanged.

H + 2-butyne and the CH_3 + propyne transition states as free rotors, branching to H + 2-butyne would increase by an approximate factor of 4, but the CH_3 + propyne channel would still comprise >90% of the products. The RRKM results are presented with the caveat that our experimental results showed that a significant portion of the 2-buten-2-yl radicals survive although they are higher in energy than the CH_3 + propyne barrier. Figure 4 shows that some of the radicals with internal energy up to 14 kcal/mol over our experimentally determined lowest dissociation barrier can survive and be detected as stable C_4H_7 fragments. This cannot be explained by energy partitioned into rotation during the initial C−Cl bond fission or by the 2.5 kcal/mol carried away in $Cl(^2P_{1/2})$. Also, we have postulated that our higher internal energy radicals are in a low-lying excited state of 2-buten-2-yl; the RRKM calculations are not relevant to the dissociation of the excited-state radicals.

We have explicitly tested the predictions of such RRKM calculations against our experimental results for a related system, the 1-buten-2-yl radical[17] to determine the change in product branching with internal energy in the radical. Both the experimental data and RRKM results indicate that the methyl + allene channel is dominant for dissociation of 1-buten-2-yl. The energy barrier for this channel is predicted to be 5 kcal/mol lower than the barriers of the H + 1,2-butadiene and H+ 1-butyne channels. Branching to C−H fission begins to dominate at radical internal energies above 50 kcal/mol. Overall, the change in relative branching to the C−C versus C−H fission channel of the 1-buten-2-yl radical observed experimentally was in very good agreement with the RRKM predictions for the ground-state radicals.

The problem remains that we cannot compare RRKM predictions to our experimental data in the dissociation of the 2-buten-2-yl radical. The absolute photoionization cross sections of 2-butyne and 1,2-butadiene are not currently known. Relative photoionization cross sections could be determined by compar-

ing the signal from photoionization of molecular beams of 2-butyne, 1,2-butadiene and propyne. Due to time restrictions on the apparatus, we did not take high-resolution $m/e = 54$ and 40 TOF data on the same day in order to get an estimate of the C_4H_6/propyne branching ratios under identical beam conditions.

Discussion

Photolysis of 2-chloro-2-butene at 193 nm resulted in both C−Cl bond fission and HCl elimination. C−Cl bond fission produced 2-buten-2-yl radicals, some of which had sufficient internal energy to overcome the barriers to dissociation of the radical via C−C bond fission and C−H bond fission. Methyl and propyne fragments were detected as products of this dissociation, as well as C_4H_6 that could be attributed to the C−H bond fission of 2-buten-2-yl. HCl elimination from 2-chloro-2-butene produced C_4H_6 cofragments, some of which dissociated to produce methyl + propargyl radicals.

A. Experimental Determination of the Lowest-Energy Dissociation Barrier. The data presented here allow for a determination of the lowest barrier to 2-buten-2-yl dissociation as the Cl atom TOF (Figure 3) determines the internal energy of all nascent 2-buten-2-yl radicals and the signal fit in Figure 6 indicates which of the radicals survive secondary dissociation. The internal energy, E_{int}, of the 2-buten-2-yl radical is obtained by energy conservation:

$$E_{parent} + h\nu = D_0(C{-}Cl) + E_{int} + E_{Cl} + E_T$$

$h\nu$, the energy of a 193.3 nm photon, is equal to 147.8 kcal/mol, including the air-to-vacuum correction. To find D_0(C−Cl), we performed ab initio G2M(RCC, MP2) calculations on 2-chloro-2-butene and the Cl atom; and G2M(RCC6) on the 2-buten-2-yl radical. These methods[4] gave a result of D_0(C−Cl) = 93.5 kcal/mol. E_{parent} is the energy of the 2-chloro-2-butene molecule; we estimated it by assuming that vibrational modes are not cooled by the nozzle expansion and have equilibrated to the nozzle temperature. Using vibrational modes calculated at the B3LYP/6-31G(d) level of theory, the average vibrational energy of the 2-chloro-2-butene molecule was determined to be 2.5 kcal/mol at the 42.7 °C nozzle temperature for these particular data. E_{Cl} refers to the energy of the spin−orbit state of the chlorine atoms. E_{Cl} is 0 kcal/mol if Cl is produced in the $^2P_{3/2}$ state and 2.5 kcal/mol in the $^2P_{1/2}$ state.[18] Our experiments cannot distinguish between the two spin−orbit states, but 235 nm photolysis of 2-chloro-2-butene with REMPI detection in separate experiments revealed that both Cl($^2P_{3/2}$) and Cl($^2P_{1/2}$) are produced.[19] According to Figure 4, $E_T = 26 \pm 1$ kcal/mol marks the onset of dissociation of the radicals. Assuming $E_{Cl} = 0$ kcal/mol, the barrier to 2-buten-2-yl dissociation is experimentally determined to be $E_{int} = 31 \pm 2$ kcal/mol. This is in agreement with the G3//B3LYP predicted barrier to reaction 2 of 32.8 ± 2 kcal/ mol,[3] as shown in Figure 2. Note that the experimentally determined barrier is dependent on a good bond energy D_0; indeed, errors in the two may fortuitously cancel each other.

There is a notable overlap between the low E_T and high E_T distributions in Figure 4. We attempted to fit the $m/e = 55$ data in Figure 6 with a sharp cutoff between the distributions for the stable and unstable 2-buten-2-yl radicals, but could not obtain a satisfactory fit. Although one might try to explain the stability of the 2-buten-2-yl radicals from the lower E_T event by the partitioning of energy to rotation in the C−Cl bond fission, our calculations show that an impulsive C−Cl bond fission from the equilibrium geometry is not expected to partition much energy into rotation of the 2-buten-2-yl radical. Using structural parameters of 2-chloro-2-butene determined at the B3LYP/6-31G(d) level of theory, we estimated the rotational energy to be 1.2 kcal/mol for the trans- isomer and 0.2 kcal/mol for the cis- isomer at an E_T of 11 kcal/mol, the lowest E_T possible for surviving 2-buten-2-yl radicals.

B. Excited- and Ground-State Dynamics of C−C Bond Fission in 2-Buten-2-yl Radicals. The dissociation of 2-buten-2-yl → CH_3 + propyne, reaction 2, is peculiar in that it could not be fit simply by the $P(E_T)$ for unstable 2-buten-2-yl radicals coupled with a single secondary $P(E_T)$ for the kinetic recoil of methyl + propyne. The data required a $P(E_T)$ that peaked at 1 kcal/mol to describe the recoil of CH_3 + propyne from the lowest E_T, higher internal energy 2-buten-2-yl radicals, and a second $P(E_T)$ peaked at 6 kcal/mol to describe the dissociation of the higher E_T, lower internal energy unstable 2-buten-2-yl radicals. This suggests that the two different distributions of 2-buten-2-yl radicals are dissociating by different mechanisms. Recent EOM-CCSD/6-31+G* calculations by Levchenko and Krylov on the excited states of the *trans*-2-buten-2-yl conformer found a vertical $^2(\pi\rightarrow n)$ transition of 3.6 eV, with $\Delta E = 2.5 \pm 0.2$ eV (57.6 ± 5 kcal/mol) energy difference at the equilibrium geometry of the lowest excited state without zero-point corrections.[20] In our experiment, the unstable 2-buten-2-yl radicals from C−Cl fission imparting 0−7 kcal/mol in product translation were the ones that evidenced the very distinct C−C bond fission exit channel dynamics, imparting little energy to recoil kinetic energy between the methyl and propyne products. These radicals have internal energies ranging from 50 to 57 kcal/mol. We conclude that unlike the lower internal energy radicals, which evidence C−C bond fission dynamics consistent with the 9.3 kcal/mol predicted exit barrier on the ground-state potential energy surface, these higher internal energy radicals are likely found in the excited state. Within the error of our calculation of E_{int} for the 2-buten-2-yl radicals (which relies on a C−Cl bond energy calculation for the precursor), our result is in rough agreement with the lowest excited-state having energy equal to or lower than the result of Levchenko and Krylov. Low E_T, high internal-energy unstable 2-buten-2-yl radicals are formed in the $^2(\pi\rightarrow n)$ excited state, while the higher E_T radicals are formed in the ground electronic state, resulting in two different distributions for energy release in the recoil of CH_3 + propyne. More recent 3rd order H^{ν} calculations[21] with a DZP + Diffuse basis set[22] found a vertical excitation energy of 1.75 eV and an oscillator strength of 0.00062 for the lowest excited state of *trans*-2-buten-2-yl. The computational method has been described previously.[23] The excited state was assigned to a $^2(\pi\rightarrow n)$ transition.

C. Benchmarking Electronic Structure Calculations on Radicals. One value of the experiments presented here is to benchmark emerging electronic structure calculations of the energetics of the barriers predicted for reactions involving radical species. Referring back to Figure 1, we note that these experiments on the 2-buten-2-yl radical have determined that the zero-point corrected barrier of dissociation to methyl + propyne is 31 ± 2 kcal/mol. This is in very good agreement with the G3//B3LYP predicted barrier of 32.8 ± 2 kcal/mol. The good agreement between experiment and theory relies on the G3 correction to the energy; without the G3 correction, the B3LYP predicted barrier is 36.0 kcal/mol using a 6−31(d) basis. (All barriers include a zero-point correction.)

The same conclusions were reached in two other experimental studies from this laboratory.[14,24] These studies examined the barriers to the two competing C−H fission channels of

2-propenyl radicals and showed conclusively that the zero-point corrected barrier to the H + propyne dissociation products is lower than that for the H + allene product channel by 1−2 kcal/mol, in agreement with G2//B3LYP. Without the G2 correction, the predicted barrier for the H + allene channel is lower than that for the H + propyne channel, inconsistent with the experimental results, and even the relative heats of formation of allene and propyne are not well predicted.[25] Though the overlapping signal from HCl elimination products did not allow us to experimentally determine the lowest C−H bond fission barrier, in our recent work[17] on the unimolecular dissociation of another C_4H_7 radical, 1-buten-2-yl, the experiments established that the barrier to C−H fission to form H + 1-butyne was higher than the C−C fission barrier to form CH_3 + allene by 5 ± 2 kcal/mol, also in agreement with the theoretical prediction from the G3//B3LYP calculations.

D. Relevance to Bimolecular Reaction Kinetics. The experimental results presented here and the theoretical predictions summarized in Figure 1 also offer insight into bimolecular addition reactions that proceed through radical intermediates. Of particular relevance are the CH_3 + propyne reaction and the H + 1,2-butadiene reaction. For the CH_3 + propyne reaction, our results are consistent with the entrance channel barrier deduced from early kinetic measurements of Getty et al.[9] Their kinetic data were fit to an Arrhenius expression and yielded an activation energy of 8.8 kcal/mol. Our previous G3//B3LYP calculations predicted a zero-point corrected entrance channel barrier of 9.3 ± 2 kcal/mol, while our experimentally measured onset of that channel corresponds to an entrance channel barrier for that reaction of 7.5 ± 2 kcal/mol. Simple reactive hard-sphere models[26] suggest that the E_a determined from kinetic data is 1/2 kT larger than the zero-point corrected barrier height, so the experimentally determined activation energy of 8.8 kcal/mol deduced by Getty suggests a zero-point corrected barrier of 8.4 kcal/mol. This is very close to our experimentally determined barrier, lower by only 1 kcal/mol than the G3//B3LYP prediction and well within the error bars of both determinations. In contrast, recent electronic structure calculations at the W1h//QCISD/6-31G(d) level of theory by Radom and co-workers[27] suggest the CH_3 + propyne reaction has a zero-point corrected barrier of 11 kcal/mol, somewhat higher than both our experimental estimate and that of Getty, although within the error bars of the G3//B3LYP estimate. (Radom's work also reported a reanalysis of Getty's kinetic data, modeling the preexponential factor differently, that suggested that Getty's data were better fit by an activation energy of 9.46 kcal/mol.)

Armed with the now experimentally validated transition state energetics for addition reactions proceeding through the 2-buten-2-yl and 1-buten-2-yl radical intermediates, one can make a number of predictions for the mechanism and product branching of the H + 1,2-butadiene reaction and critique early assumptions about this reaction. The only experimental study of the kinetics of this reaction reported on the NIST Chemical Kinetics Database is the one by Kern and co-workers.[28] Those researchers were studying the pyrolysis of 1,2-butadiene, so their kinetic model included rate parameters for some elementary reactions to which their data were not particularly sensitive, in retrospect. The Kern et al. paper suggests the two dominant reaction products of the reaction of H + 1,2-butadiene are an H-atom abstraction reaction to form H_2 + 1,2-butadienyl radical and a reaction channel forming vinyl + ethylene. The experimental results presented in this paper, combined with the theoretical predictions summarized in Figure 1 and the experimental work in ref 17, suggest that Kern's conclusions about this elementary reaction are dramatically in error. Figure 1 shows that three radical intermediates are possible when the H atom adds to 1,2-butadiene: methylallyl, 1-buten-2-yl and 2-buten-2-yl. Figure 1 also suggests that the addition reaction to form the 2-buten-2-yl radical has the lowest of the three barriers and would dominate at low collision energies. (G2//B3LYP calculations by Laskin, Wang and Law in 2000 mapped out two of these pathways but missed the third, and did not report the differing entrance channel barrier heights.[2]) The difference in the three barriers for the addition reaction does not result from tightened modes at the transition states, as there is no significant difference in the zero-point energy at the three transition states. It is clear that the dominant products of the reaction of H + 1,2-butadiene at low temperature should be CH_3 + propyne, the lowest barrier decomposition products of the radical detected in the experiments presented in this paper, not vinyl + ethylene or H_2 + 1,2-butadienyl radical as suggested by Kern. At higher temperatures, one would expect contributions from H + 1,3 butadiene to contribute to the product branching (from the H atom addition to form the methylallyl radical intermediate) and methyl + allene products from the addition proceeding through the 1-buten-2-yl radical intermediate, with a small contribution from 1-butyne + H products at higher energies. The only route to form Kern's deduced products of vinyl + ethylene is through the 3-buten-1-yl radical, which is not formed in the addition of an H atom to 1,2 butadiene (it is formed in the addition of an H atom to 1,3-butadiene). Only one of the three possible radical intermediates formed from the addition of H atoms to 1,2-butadiene, the 1-methylallyl radical, might isomerize with any substantial efficiency to the 3-buten-1-yl radical intermediate that does give Kern's proposed vinyl + ethylene product channel, but the rate of isomerization of the 1-methylallyl radical to the 3-buten-1-yl radical is much slower than the rate for it simply to dissociate to H + 1,3-butadiene. Studying Kern's analysis further reveals that he had little reason to infer the two product channels he includes for H + 1,2-butadiene; indeed the paper states that the rate parameters assigned for these inferred reactions are "comparable to those of similar 1,3-butadiene reactions" reported by Keifer.[29] Our analysis shows, however, that while the vinyl + ethylene product channel would occur in the reaction of H + 1,3 butadiene as proposed by Keifer, it would not contribute to any significant extent in the reaction of H with 1,2-butadiene.

Indeed, later kinetics studies on 1,2-butadiene, 2-butyne and 1,3 butadiene pyrolysis in shock tubes also made a dramatically different assumption than Kern did on the product branching in the H + 1,2-butadiene elementary reactions involved in the mechanisms. In particular, these later studies no longer assumed that vinyl + ethylene was the dominant product in the elementary reaction of H + 1,2-butadiene. In analogy with H + allene, they assumed that the reaction of H + 1,2-butadiene yields primarily CH_3 + allene[30] and later[31,32] added the CH_3 + propyne product channel, assuming its rate was identical to that producing CH_3 + allene. These guesses are in much better accord with the present study, with the exception that they assumed the activation energy and Arrhenius preexponential factor for the reaction producing CH_3 + propyne are identical to those for producing CH_3 + allene. The very recent theoretical work of Miller discussed in our present experimental study suggests the reaction producing CH_3 + allene, via the 1-buten-2-yl radical intermediate, has a considerably larger entrance channel barrier from the H + 1,2-butadiene reactant than does the CH_3 + propyne product channel, which proceeds through the 2-buten-2-yl radical studied here. Note that the isomerization barrier between these two radical isomers is higher than the

exit channel barriers leading to the $CH_3 + C_3H_4$ products, so we expect the CH_3 + propyne product channel to dominate if the theoretical prediction for the relative entrance channel barriers is correct. Only the methylallyl radical intermediate has an isomerization channel that might affect the product branching in the H + 1,2-butadiene elementary reaction.

Bulk thermal decomposition of 1,2-butadiene, 2-butyne and 1,3-butadiene has been studied by Chambreau et al.[33] and Hidaka et al.[32] In the pyrolysis of 1,3-butadiene and 2-butyne, both papers noted the importance of isomerization to 1,2-butadiene followed by dissociation to CH_3 + propargyl. The results show that although 1,2-butadiene can isomerize to other C_4H_6 isomers, dissociation to CH_3 + propargyl is much more likely than isomerization. In our experiments, it is important to note that H loss from 2-buten-2-yl produces 1,2-butadiene or 2-butyne, neither of which would have enough energy to overcome the barriers[32,33] of the isomerization or decay channels. The C_4H_6 cofragments formed in HCl elimination from the photolytic precursor, however, could access these channels, a point we considered in our analysis.

Thus, the experiments presented here offer a way to probe key transition states in both the unimolecular dissociation reactions of isomerically selected radicals and to probe bimolecular reactions of H atoms and methyl radicals with unsaturated hydrocarbons that proceed through these radical intermediates. One caution in developing predictive ability for the bimolecular reactions is, however, that there is the implicit assumption that the reaction proceeds via an initial addition to form the corresponding radical intermediate. Though this assumption is expected to be quite good for the systems studied here, for reactions such as $O(^1D)$ + methane it has been shown that the reaction proceeds through both direct and the long-lived intermediate pathways;[34] then studies of the unimolecular dissociation of the intermediate would only probe the latter pathway for the bimolecular reaction.

Acknowledgment. This work was supported by the National Science Foundation, Grant CHE-0403471. The Advanced Light Source is supported by the Director, Office of Science, Office of Basic Energy Sciences, Materials Sciences Division, of the U.S. Department of Energy under Contract No. DE-AC03-76SF00098 at Lawrence Berkeley National Laboratory. The Chemical Dynamics Beamline is supported by the Director, Office of Science, Office of Basic Energy Sciences, Chemical, Geosciences and Biosciences Division, of the U.S. Department of Energy under the same contract. L.R.M. was partially supported by a U.S. Department of Education GAANN Fellowship. Doran Bennett is acknowledged for executing the G2M(RCC) calculations reported here. The authors thank William McDaniel of Narchem Corporation for assistance in obtaining and shipping 2-chloro-2-butene samples.

References and Notes

(1) Matheu, D. M.; Green, W. H., Jr.; Grenda, J. M. *Int. J. Chem. Kinet.* **2003**, *35*, 95.

(2) Laskin, A.; Wang, H.; Law, C. K. *Int. J. Chem. Kinet.* **2000**, *32*, 589.

(3) Miller, J. L. *J. Phys. Chem. A* **2004**, *108*, 2268.

(4) Mebel, A. M.; Morokuma, K.; Lin, M. C. *J. Chem. Phys.* **1995**, *103*, 7414.

(5) Frisch, M. J.; G. W. T.; Schlegel, H. B.; Scuseria, G. E.; Robb, M. A.; J. R. C.; Zakrzewski, V. G.; Montgomery, J. A., Jr.; Stratmann, R. E.; J. C. B.; Dapprich, S.; Millam, J. M.; Daniels, A. D.; K. N. K.; Strain, M. C.; Farkas, O.; Tomasi, J.; Barone, V.; M. C.; Cammi, R.; Mennucci, B.; Pomelli, C.; Adamo, C.; Clifford, S.; J. O.; Petersson, G. A.; Ayala, P. Y.; Cui, Q.; Morokuma, K.; N. R.; Salvador, P.; Dannenberg, J. J.; Malick, D. K.; Rabuck, A. D.; K. R.; Foresman, J. B.; Cioslowski, J.; Ortiz, J. V.; A. G. B.; Stefanov, B. B.; Liu, G.; Liashenko, A.; Piskorz, P.; I. K.; Gomperts, R.; Martin, R. L.; Fox, D. J.; Keith, T.; M. A. A.-L.; Peng, C. Y.; Nanayakkara, A.; Challacombe, M.; Gill, P. M. W.; B. J.; Chen, W.; Wong, M. W.; Andres, J. L.; Gonzalez, C.; M. H.-G.; Replogle, E. S.; Pople, J. A. *Gaussian 98*, Revision A.11.3; Gaussian, Inc.: Pittsburgh, 2002.

(6) Lee, H.-Y.; Kislov, V. V.; Lin, S.-H.; Mebel, A. M.; Neumark, D. M. *Chem. Eur. J.* **2003**, *9*, 726.

(7) Dewar, M. J. S.; Olivella, S. *J. Am. Chem. Soc.* **1979**, *101*, 4958.

(8) Stein, S. E.; Rabinovitch, B. S. *J. Phys. Chem.* **1975**, *79*, 191.

(9) Getty, R. R.; Kerr, J. A.; Trotman-Dickenson, A. F. *J. Chem. Soc. A* **1967**, 1360.

(10) Yang, X. M.; Lin, J.; Lee, Y. T.; Blank, D. A.; Suits, A. G.; Wodtke, A. M. *Rev. Sci. Instrum.* **1997**, *68*, 3317.

(11) Heimann, P. A.; Koike, M.; Hsu, C. W.; Blank, D.; Yang, X. M.; Suits, A. G.; Lee, Y. T.; Evans, M.; Ng, C. Y.; Flaim, C.; Padmore, H. A. *Rev. Sci. Instrum.* **1997**, *68*, 1945.

(12) Peterka, D.; Ahmed, M., Personal Communication.

(13) For details, see: Person, M. D. Ph.D. Thesis, University of Chicago, Chicago, 1991.

(14) Mueller, J. A.; Parsons, B. F.; Butler, L. J.; Qi, F.; Sorkhabi, O.; Suits, A. G. *J. Chem. Phys.* **2001**, *114*, 4505.

(15) Lias, S. G.; Bartmess, J. E.; Liebman, J. F.; Holmes, J. L.; Levin, R. D.; Mallard, W. G. Ion Energetics Data. In *NIST Chemistry WebBook, NIST Standard Reference Database Number 69*; Linstrom, P. J., Mallard, W. G., Eds.; National Institute of Standards and Technology: Gaithersburg, MD, 2003.

(16) Hase, W. L.; Bunker, D. L. *QCPE* **1974**, *234*.

(17) Miller, J. L.; Krisch, M. J.; Butler, L. J.; Shu, J. *J. Phys. Chem. A* **2005**, *109*, 4038.

(18) Kelly, R. L. *J. Phys. Chem. Ref. Data* **1987**, *16*, Supplement 1.

(19) Liu, Y.; Butler, L. J., Manuscript in preparation.

(20) Levchenko, S.; Krylov, A. Personal communication of work in progress, Nov. 8, 2004.

(21) Perrine, T.; Freed, K. F. Personal communication, April 28, 2005.

(22) Dunning, T. H.; Hay, P. J. In *Modern Theoretical Chemistry Vol. 3: Methods of Electronic Structure Theory*; Schaefer, H. F., III, Ed.; Plenum Press: New York, 1977.

(23) Chaudhuri, R. K.; Majumder, S.; Freed, K. F. *J. Chem. Phys.* **2000**, *112*, 9301.

(24) Mueller, J. A.; Miller, J. L.; Butler, L. J.; Qi, F.; Sorkhabi, O.; Suits, A. G. *J. Phys. Chem. A* **2000**, *104*, 11261.

(25) Muckerman, J. T. Personal communication, July 15, 2004.

(26) Houston, P. L. *Chemical Kinetics and Reaction Dynamics*; McGraw-Hill: New York, 2001.

(27) Gomez-Balderas, R.; Coote, M. L.; Henry, D. J.; Fischer, H.; Radom, L. *J. Phys. Chem. A* **2003**, *107*, 6082.

(28) Kern, R. D.; Singh, H. J.; Wu, C. H. *Int. J. Chem. Kinet.* **1988**, *20*, 731.

(29) Keifer, J. H.; Wei, H. C.; Kern, R. D.; Wu, C. H. *Int. J. Chem. Kinet.* **1985**, *17*, 225.

(30) Hidaka, Y.; Higashihara, T.; Ninomiya, N.; Oshita, H.; Kawano, H. *J. Phys. Chem.* **1993**, *97*, 10977.

(31) Hidaka, Y.; Higashihara, T.; Ninomiya, N.; Oki, T.; Kawano, H. *Int. J. Chem. Kinet.* **1995**, *27*, 331.

(32) Hidaka, Y.; Higashihara, T.; Ninomiya, N.; Masaoka, H.; Nakamura, T.; Kawano, H. *Int. J. Chem. Kinet.* **1996**, *28*, 137.

(33) Chambreau, S. D.; Lemieux, J.; Wang, L.; Zhang, J. *J. Phys. Chem. A* **2005**, *109*, 2190.

(34) Yu, H.-G.; Muckerman, J. T. *J. Phys. Chem. A* **2004**, *108*, 8615.